One-dimensional pilot-wave dynamics of walking droplets

Author:
Sebastiaan Koerhuis
Utrecht University

Bachelor Thesis: *Physics & Astronomy*

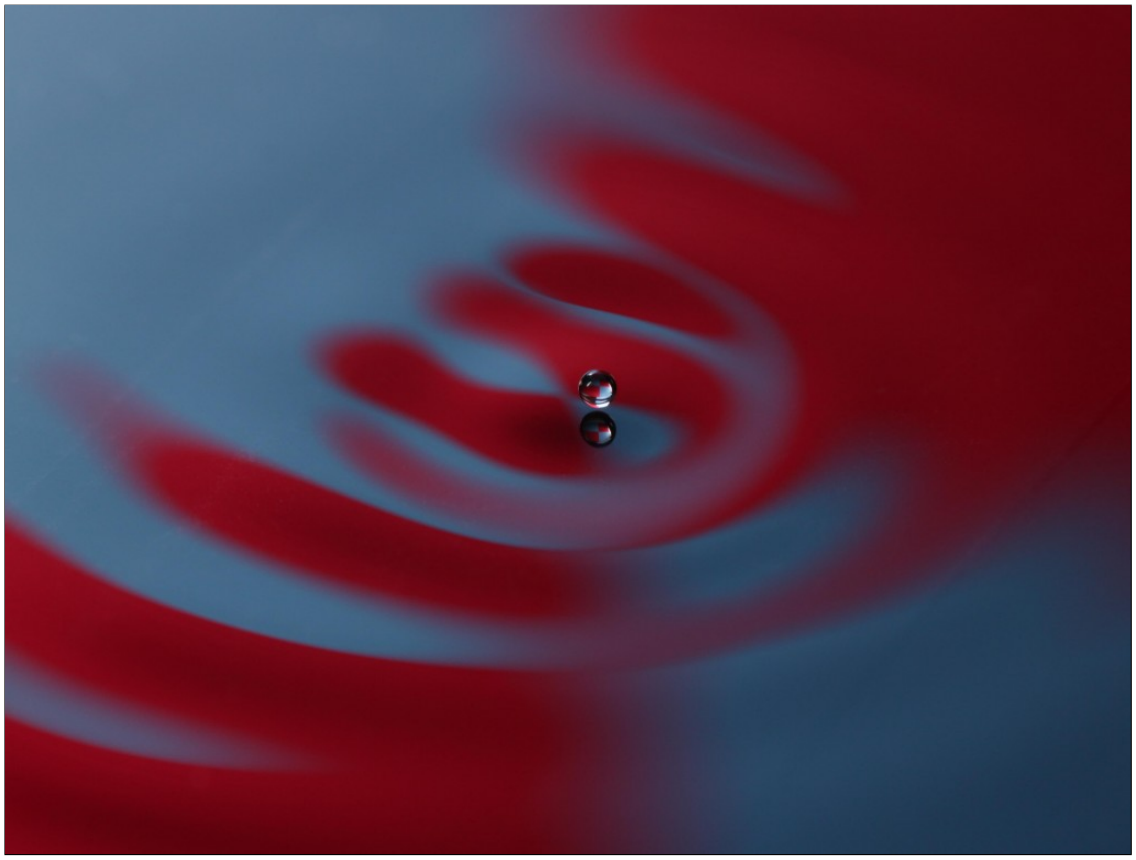
[1]

Supervisors:
Prof. dr. L.R.M. (Leo) Maas
Utrecht University

Prof. dr. P. (Peter) van der Straten
Utrecht University

June 12, 2020

Abstract

Pilot-wave dynamics of walking droplets is a field in hydrodynamics that has been studied extensively for its interesting features previously thought to be found only in quantum mechanics. The walking droplets in combination with their pilot-wave form a spatially delocalized entity called a walker, wherefrom quantum-like features arise.

The behavior and dynamics of the droplet have been described theoretically, where the walker moves in a two-dimensional (plane) bath. We start the theoretical development of an analogous one-dimensional version of this theory that describes the walker's behavior in an one-dimensional (long and narrow) bath. We set up the model basis for the equation of motion of the vertically bouncing droplet by looking at a quasi-static droplet in our one-dimensional system.

Our goal is to develop a theory that eventually describes and rationalizes the dynamics and statistical behavior of a walker in our one-dimensional setting. We predict that the simplification to an one-dimensional setting will make the theory behind the behavior of the walker system more understandable. Hence, the theory, which is the basis for explaining the emerging quantum-like features, will eventually shed some light on what is and what is not fundamental to quantum mechanics.

Specifically, the surface- and potential energy of a quasi-static droplet are calculated and expressed in an harmonic decomposition of the droplet's shape. The expansion coefficients that arise in the harmonic decomposition are calculated by performing an averaging method on the potential energy and minimizing the total energy of a droplet resting on a rigid surface. The expansion coefficients are shown to accurately describe the droplet's shape for a range of Bond numbers (a dimensionless number representing the relative magnitude of gravity to surface tension per unit area), where the range depends on the contact area that the droplet makes with the underlying surface. These results can be used to further develop the one-dimensional walker theory.

Contents

1 Introduction

Imagine a spherical droplet of millimetric size falling on a slightly vibrating fluid bath at low speed (Fig. 1). The vibration is caused by a driving piston underneath the bath, which vertically moves the bath at an amplitude and frequency just *below* the Faraday threshold. Above this threshold, a pattern of standing waves will appear in the bath, which are called Faraday waves [2]. If the system parameters are just in the right range, the droplet will not coalesce with the bath, but it will start to bounce back. It may either stay put at its horizontal location, or, when perturbed for instance by wind, it may "walk"across the bath at a speed of 1cm/s. During its bounces, at every impact the droplet makes, it creates waves which at the same time act as a guide for the walking droplet, for if the droplet falls onto a sloping side of the previously generated wave, the wave steers it forward. The wave field thus acts as a pilot-wave to the walking droplet. The combination of the walking droplet and the pilot-wave is a spatially delocalized entity called a walker. Couder and colleagues found this walker system experimentally [3]. Experiments and theoretical considerations explored several quantum-like features of the walker system, often assumed to be only found in quantum mechanical systems [1, 4]. Depending on one's knowledge of quantum mechanics, these quantum-like features may or may not be surprising to find in the walker system. For example, the walkers are able to tunnel across a fluid layer on top of a barrier [5]. These quantum-like features find their root in the spatial delocalized character of the walker and may shed light on the dynamics of delocalized particle-wave systems.

A theory describing the walker system has already been completed and investigated [6, 7]. The theory shows that the walker system is a deterministic system, meaning that the theory can predict what the walker will do in the *immediate* future. The theory describes the bath deformation and the droplet's trajectory in a two-dimensional setting. The two-dimensional setting refers to the fluid bath extending in two horizontal dimensions, the x- and y-direction, where the droplet is of approximately spherical shape.

Now, our goal is to make a similar theoretical development of the walker system in a simplified one-dimensional setting. The one-dimensional setting refers to a bath extending in the x-direction, and extending just enough in the y-direction for a *cylindrical* droplet to fit between the bath's boundaries. The fluid bath is sufficiently longer in the x-direction than in the y-direction, so that the dynamics of the wave field and the droplet are only to be considered in the x-direction. The dynamics of this system will have one-dimensional waves and a droplet hopping from left to right through the air.
Such a theoretical development will, when it is completed, predict and rationalize the dynamical and statistical behavior of the simplified walker system when the walker is observed in an experimental setting. Therefore, this theory will also rationalize and shed some light on quantum-like features of this walker system.

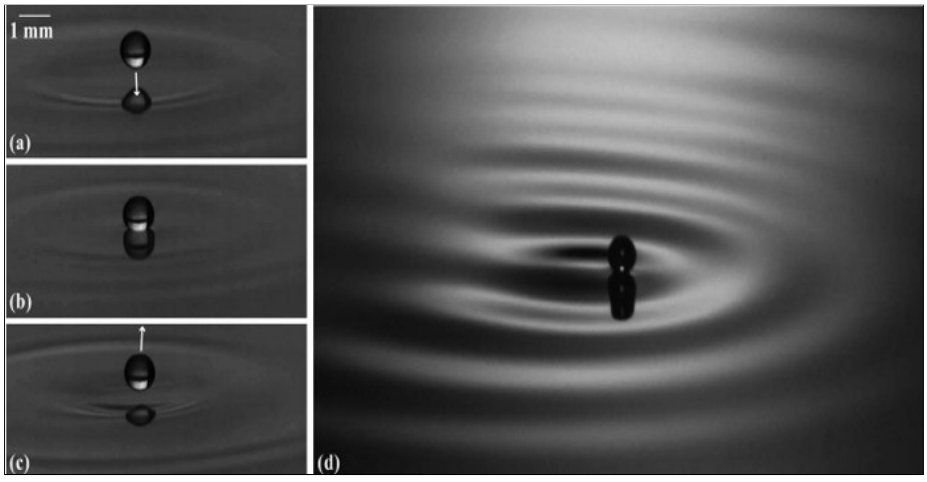

Figure 1: A droplet of spherical size interacting with a vibrating fluid bath; (a) the droplet is falling to the bath due to gravity. (b) the droplet interacts with the bath and creates a wave. (c) the droplet bounces away from the bath. (d) the droplet is walking across the bath [6].

There are two main reasons why it is interesting to simplify the walker system and look at the resulting dynamics:

- First of all, pilot-wave theories serve as a macroscopic analog to quantum mechanics to the extent that it gives a conceptual framework for understanding results in quantum mechanics through a mechanistic lens [1]. Such a framework is not provided by the purely statistical interpretation of quantum mechanics. The simplified version of the walker system will make the conceptual framework more accessible for readers with a basic understanding of quantum mechanics. Most undergraduate quantum mechanics courses start with one-dimensional examples like the harmonic oscillator, or the infinite square well. It makes sense that the conceptual framework should also be one-dimensional.

- Secondly, undergraduate courses on quantum mechanics, at least in my experience, shows the student how to *do* quantum mechanics, but spend little time on what quantum mechanics *means*. I am sure this is for good reason. If the student starts by learning the mathematical formalism of quantum mechanics, he or she has a stronger basis for understanding quantum mechanical results and not misinterpret these with their classical intuition. The simplified walker system will leave less room for such misinterpretation compared to a more complex two-dimensional walker system, because the theory and the behavior of the simplified walker system will be easier to understand. In the same way, the simplified theory will make it clearer where in the theory these quantum-like features will arise. Therefore, traits that are at the core of quantum mechanics, which are only found in quantum mechanical experiments, become apparent. These core properties then also become more distinct from quantum-*like* features found in the simplified walker system.

This thesis confines itself to the setup and start of the theory for the simplified walker system. Consequently, the dynamics and statistical behavior of the walker has not been predicted and rationalized yet. We hope to inspire some reader or interested fellow student to pick up where our development stops and complete or add to the theory.

The mechanics and setup of the walker system are explained in more depth in section 2. Also, an example of a two-dimensional walker system with quantum-like features will be shown and elaborated on. In section 3, a start to the theory of the simplified one-dimensional walker system is given. After that, a guideline on how to complete the theory in lign with its two-dimensional analog is given for the inspired reader. In section 4, we conclude this thesis and discuss some points about the theory we have developped and the chaotic nature of the walker system. Finally, in section 5, I give my thoughts on quantum interpretations.

2 The walker system

2.1 Mechanics and behavior

The walkers are very subtle entities and depend on a wide number of parameters. First of all, the fluid in the bath is characterised by its density ρ, kinematic viscosity ν, and surface tension σ. The droplet is (or can be) of the same substance as the bath and is characterised similarly. Now, the vibration of the bath is caused by a mechanical piston just below the bath and drives the bath uniformly across the area of the bath up and down. The vibration is characterised by the amplitude of the vertical motion of the bath A_0 and the frequency of the driving piston $f = \frac{\omega}{2\pi}$. These two parameters merge in $\gamma = A_0\omega^2$, the driving acceleration. Above the threshold γ_F, which is called the Faraday threshold, the bath becomes unstable to a pattern of Faraday wave fields. The walker experiments are performed at $\gamma<\gamma_F$, so that the bath stays flat, but the forcing of the bath is still noticed and critical to the walker system.
What this "critical"forcing means is that the forcing provides energy to the system and hence to the motion of the droplet and to the wavefield that results from drop impact. Also, because the forcing is uniform and has a constant frequency, the bath is set up to host a monochromatic wave field. More specifically, this setup has the effect that after impact of the droplet, when a wave moves away from the point of impact, a field of standing waves is left in the wave's wake. For there to be a standing wave, there has to be some wave propagating opposite to the direction of the wave as a result of impact, which is caused by the boundaries of the bath. This field of standing waves persists for a longer period of time if γ comes closer to the Faraday threshold.

At some point a droplet of a certain size and substance falls with an impact speed on the bath, where the system is under the influence of gravity. The droplet's behaviour has been mapped by looking at how it behaves depending on the dimensionless forcing, $\frac{\gamma}{g}$, and the vibration number, $V_i = \omega\sqrt{\frac{\rho a^3}{\sigma}}$, the relative magnitude of the forcing frequency and the drop's natural oscillation frequency. An illustrating and very informative regime diagram is shown in figure 2 in the review - *Pilot-Wave Hydrodynamics* - by Bush [1], which we highly recommend looking at for more details about differences in behaviours of the walker.

For our consideration, the droplet starts bouncing above the bouncing threshold $\gamma>\gamma_b$ for a droplet in the right size range. If γ is higher than the walking threshold γ_w, the droplet may start walking. In this walking regime, the droplet can also start walking chaotically, which happens at γ close to the Faraday threshold γ_F. Near the Faraday threshold, the standing waves do not die out quick enough for the bath to return to a quiescent form when the droplet comes back to interact with the bath again. Or put differently, near the Faraday threshold, the system will be at high-memory and the waves that propell the droplet become more important. The nonlocal essence of the walker is apparent here, because the waves propelling the droplet in the present depend on the past path the droplet took where it left a pattern of standing- or traversing waves behind. Usually after some short time, for a bath size considered in experiments, standing waves are left behind. But, for example, in an extremely large sized bath, there are no traversing waves (yet) to interfere with traversing waves going in opposite direction with the lack of boundary effects, thus no standing waves can emerge. What happens in such a case is discussed in section 4.

To come back to droplets walking chaotically, the chaotic paths the droplets follow means that one does not know where the droplets will end up eventually, because the paths are extremely sensitive to small changes in initial conditions. This does not mean that the walker system is intrinsically indeterministic. The droplet's motion can still be described by a trajectory equation [6], which is a differential equation predicting the droplets horizontal position. But just for a tiny difference in initial conditions, which is uncontrollable, the position that the trajectory equation predicts for a droplet will end up to be different.

2.2 Quantum-like features

Below, quantum-like features of a specific experiment are shown, just like Bush did in his review mentioned earlier [1]. Other quantum-like features in different experiments are also discussed in this review.

When the walker system is being examined in a circular corral, interesting statistical behaviour is found at high-memory of the system [8, 9], giving the probability to find the droplet somewhere in the corral.
High-memory is a requirement for the statistical behaviour in as much as in the lower-memory system, the statistical behaviour is not as rich and does not have analogous results to quantum corral experiments. Also, for there to be any statistical behaviour, one has to look at the long-*path*-memory of the system, indicating that enough time has passed for the droplet to be walking.
Let us now look at the corral's geometry. At high memory, walkers are moving chaotically due to the complexity of the wavefield. When the bath is confined to a corral, complexity is created by the droplet's impacts, wave reflections off the wall and the driving piston below the corral. For a circular corral, walkers in this system have the tendency to move along the azimuthal angle of the corral at certain distances radially. Hence, a statistical pattern emerges where to find the particle in the corral, which takes on the form of the amplitude of the Faraday wave mode of the corral at a certain driving forcing $\gamma > \gamma_F$. This statistical pattern is shown in Fig. 2. The cause of the walkers having "preferred"trajectories to follow is the interaction of the droplet with the underlying wave field. Namely, the droplet is found to walk between maxima of the physical wavefield and when found bouncing off the slopes of the waves, it skips (quickly) to another local minimum in the wave pattern to walk along.

Thus we see that the statistical behaviour of this corral setup is explained by the (complex) pilot-wave dynamics. The observed statistical behaviour is similar to quantum corral experiments with electrons, where the electron density on a copper substrate was found to have a similar wave like pattern as the corral shape [10, 11]. We see that the chaotic nature of the walking droplets and certainly the vast parameter setup of the system are the cause for there to be a statistical pattern. In quantum mechanics, following Born's statistical interpretation, the statisitical information is all there is to know about the particle's possible positions. Since the uncertainty principle in quantum mechanics does not allow for a deterministic description like that of the chaotic walker, the statistical behaviour does not have an analogous explanation in quantum mechanics. Finally, we can thus see that the chaotic nature of the walker in the right parameter regime is mimicking quantum results. At the same time, it becomes apparent what dynamical behaviour of the droplet is the cause for these quantum-like results.

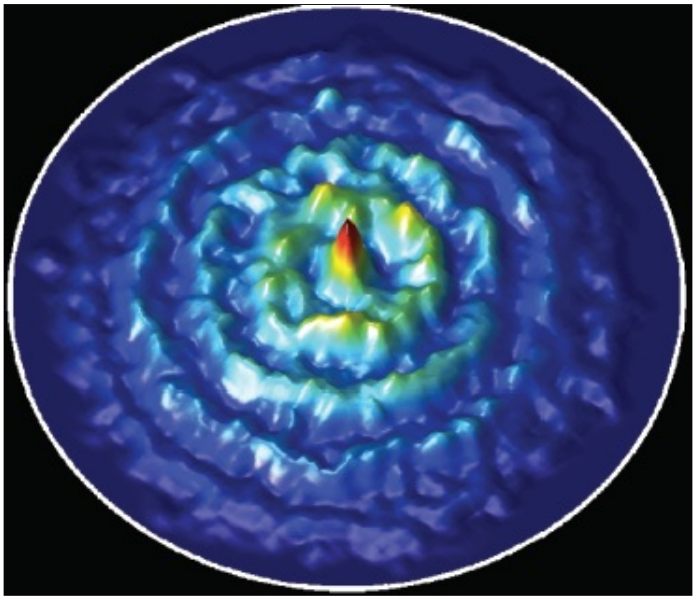

Figure 2: The probability distribution of finding the droplet at a specific position in the corral [8].

3 One-dimensional theory

To describe the motion of the walkers analytically for our one-dimensional walker system, we look at how the description has been done for the two-dimensional walker system. In three subsequent papers written by Moláček and Bush, they develop a theory for rationalizing the behaviour of bouncing and walking droplets on a vibrating bath for the two dimensional walker system [7, 12, 13]. They also compare and adjust this theory with experiments done. The first article, *A quasi-static model of drop impact - 2012*, is the article which we use as a starting point for the one-dimensional theory. Our development in this section is mostly an analog to this article. Hence if we refer to the names Moláček and Bush, this article is what we are refering to, unless indicated otherwise. The article works towards the equation of motion of a *quasi-static* droplet. What the quasi-static droplet entails will become clear in section 3.1. For a review of the theoretical modeling of the walkers, which looks at different approaches to developing a theory, see [14].

More specifically, we are going to calculate the surface- and potential energy of the quasi-static droplet in terms of system parameters and expansion coefficients b_m. The steps that follow these results in order to complete the theory are mentioned in section 3.6.

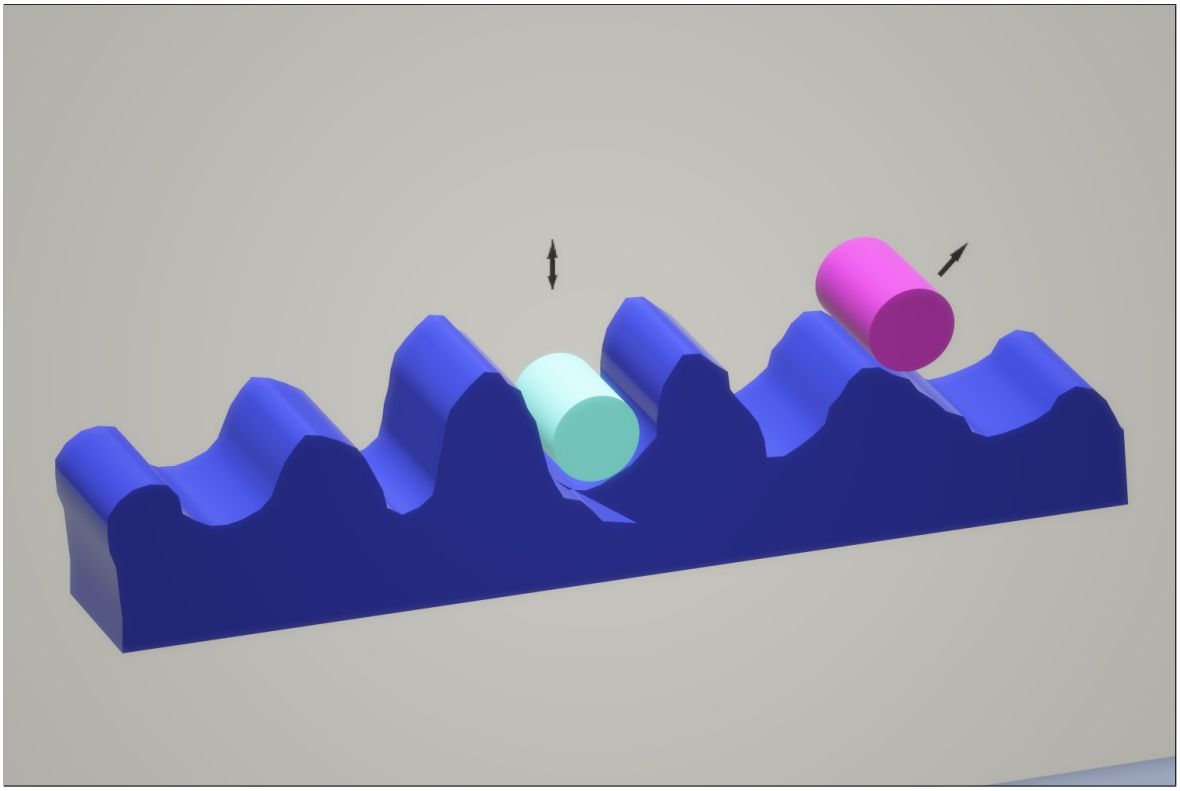

Figure 3: A physical representation of the one-dimensional walker system in a long but narrow bath. The turqouise droplet represents a droplet in a bouncing mode, bouncing only in vertical direction. The purple droplet represents a droplet in a walking mode, bouncing off wave crests and thus moving in vertical and horizontal direction.

3.1 System and droplet's parameters

We switch from a spherical droplet to a cylindrical droplet when going from the two-dimensional walker system to the one-dimensional walker system. Thus if a droplet is mentioned in this section, a cylindrical droplet is meant, unless indicated otherwise. In the same way, the shape of the silicon surface - the substrate - of the bath just below and around the droplet switches from spherical shape to cylindrical shape.

The quasi-static droplet system can be described as follows. Consider the case of a non-wetting impact of the droplet on a rigid substrate, in which a thin air layer is maintained, but now for the one-dimensional system (Fig. 4).
First of all, non-wetting means that the droplet does not wet the substrate because there is always a thin layer of air between the droplet and substrate. The interaction between the droplet and substrate is thus being communicated through the thin air layer. This communicating air layer is not taken into account, but just as Moláček and Bush did, we take this air layer to be of neglegible thickness for the situation the theory tries to rationalize.
Secondly, we can approximate the bath below the droplet to behave as a *rigid* substrate because the Weber number

$$\mathbb{W}e = \frac{\rho R_0 V_{in}^2}{\sigma}, \tag{3.1}$$

is considered to be very small ($\mathbb{W}e \ll 1$). The Weber number is the dimensionless number describing the relative magnitude of inertia to surface tension in the system. In (3.1), ρ is the droplet's density, R_0 the radius of the undeformed droplet, V_{in} the droplet's incoming speed and σ the surface tension of the droplet. As Moláček and Bush put it;

> In the $\mathbb{W}e \ll 1$ regime, when the overall rebound dynamics is slow relative to the dynamics of the typical surface waves created, one expects the surface shapes to equilibrate to some quasi-static form (see p. 607 in [13]).

Although the substrate is rigid, it can have a curvature. This curvature is assumed to be of uniform radius, thus one can imagine the substrate around the droplet to be like part of the area of a cylinder. A side view of the situation is given in Fig. 4. The influence of this curvature is incorporated by introducing the dimensionless group $\mathcal{R} = 1 - R_0/R_2$, where R_2 is the uniform radius of the substrate. In perfect analogy with Moláček and Bush, we define the curvature of a concave substrate to be negative. Note that $\mathcal{R} = 1$ for a flat surface, $\mathcal{R} \to \infty$ for a sharp pin-shaped surface and $\mathcal{R} = 0$ for a surface whose curvature matches that of the undeformed drop.

We approximate the droplet's shape to be of a quasi-static deformed cylinder when it is under the influence of a homogeneous gravitational field. So the shape of the droplet is determined by the Bond number

$$\mathbb{B}o = \frac{\rho g R_0^2}{\sigma}, \tag{3.2}$$

the dimensionless number representing the relative magnitude of gravity to surface tension per unit area in the system. For (3.2), the parameters ρ, R_0 and σ have the same interpretation as in (3.1) and g is the gravitational acceleration.

For the rest of our theoretical development, consider the case where the droplet is *sitting* on this substrate. The drop is characterised by its density ρ, surface tension σ and undeformed radius R_0. The first order deformation of such a quasi-static droplet, caused by a *weak* gravitational field g, has already been derived for the two-dimensional system [15]. A weak gravitational field means that the droplet's deformation is small so that possible rebound dynamics of a bouncing droplet is maintained.

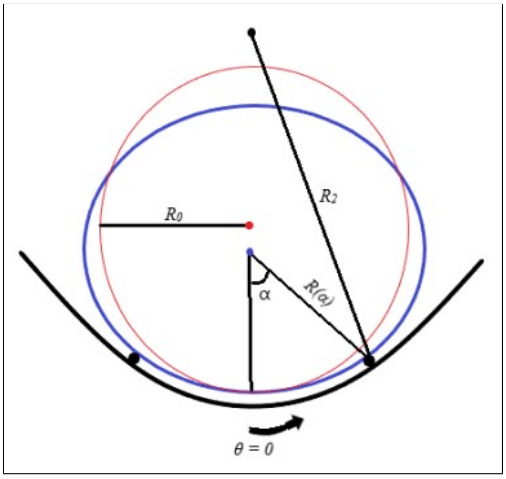

Figure 4: A cross-section of a droplet (blue) resting on a curved substrate (black), where the undeformed droplet is indicated in red. The radius of the droplet at an the angle of last contact α is indicated with $R(\alpha)$. The radius of the undeformed droplet and the substrate are indicated as R_0 and R_2, respectively.

For our one-dimensional system, the deformation of the droplet in polar coordinates is given by

$$R(\theta) = R_0(1 + \epsilon f(\theta)), \tag{3.3}$$

where $\epsilon \ll 1$. The continuous function $f(\theta)$ indicates the deformation of the drop as a function of the angle θ.

There are two points where this equation differs from its two-dimensional analog:

- The angle θ in (3.3) refers to the *polar* angle, running from 0 to 2π, starting at the bottom of the droplet (Fig. 4). In the two-dimensional analog, θ refers to the azimuthal angle and runs from 0 to π, similarly starting from the bottom of the spherical droplet.
- The function $f(\theta)$ is now a function of θ. In the two-dimensional analog, the function takes the form of $f(\cos\theta)$. This change is a consequence of the different shapes of the droplets in the one- and two-dimensional systems. When calculating the kinetic energy of both systems, f has to be written as a decomposition, which is a solution of the Laplace equation of the potential flow in the correct parameter regime. For the two-dimensional system, f has to be a solution of the *three*-dimensional Laplace equation. Hence f can be decomposed into spherical harmonics in terms of Legendre polynomials $P_m(\cos(\theta))$. For the one-dimensional system, f has to be a solution of the *two*-dimensional Laplace equation. Therefore, f can be decomposed in harmonics, an expansion in $\cos(m\theta)$.

As already mentioned, θ runs counterclockwise and starts at the bottom of the droplet. We choose the center of our coordinate system to coincide with the center of the deformed droplet, indicated with the blue dot in Fig. 4. Also, the droplet's shape has the same form as the underlying substrate in the region $-\alpha \leq \theta \leq \alpha$, in approximation. The droplet cannot have the exact same form as the substrate, because a discontinuity in $f(\theta)$ arises at the points ($\theta = \alpha$ and $\theta = -\alpha$) where the droplet stops conforming exactly to the shape of the substrate. The air layer between $\theta = \alpha$ and $\theta = -\alpha$ is approximated *theoretically* to not be there, so the droplet makes last contact with the surface at these angles.

Furthermore, we can relate α to the relative contact area δ, which is the ratio between the actual contact area and the maximum contact area ($= \pi R_0 L$), as follows

$$\delta = \frac{2\alpha}{\pi} \tag{3.4}$$

The above equation is useful in the remainder of this thesis because it is a measure for the contact area that is only dependent on one variable explicitely, the angle of last contact α.

3.2 Surface Energy

When the droplet is sitting on the substrate, the droplet becomes deformed because of the gravity pulling it down towards the substrate. We assume the droplet to deform symmetrically to the left and right from the vertical axis penetrating the top of the droplet, going through the center of mass and thus the center of our coordinate system, towards the lowest point of the droplet where $\theta = 0$. This assumption is justified because the substrate's curvature is also symmetric about the vertical axis, and the gravitational field is homogeneous.
When the droplet comes to sit to rest, the perimeter of the droplet in the new deformed state is *greater* than the perimeter of the undeformed droplet. As a consequence of this positive change of perimeter, the energy stored in the droplet increases because the molecules on the surface of the droplet are being pulled apart, which is not the preferred natural state of the molecules. Hence the new surface energy of the deformed droplet must be found.
The surface energy can be calculated by considering the geometry of the deformed droplet

$$\begin{aligned}
\mathcal{S.E.} &= \sigma \int dA \\
\mathcal{S.E.} &= \sigma \int_0^L dy \int_0^{2\pi} \sqrt{R^2 + R'^2}\, d\theta \quad \rightarrow R' = \frac{dR}{d\theta} \\
\mathcal{S.E.} &= \sigma L \int_0^{2\pi} \sqrt{R^2 + R'^2}\, d\theta.
\end{aligned} \tag{3.5}$$

Using (3.3) for R and realizing $R' = R_0 \epsilon f'$, where $f' = \frac{df}{d\theta}$, yields

$$\begin{aligned}
\mathcal{S.E.} &= \sigma L \int_0^{2\pi} \sqrt{R_0^2 + 2R_0^2 \epsilon f + R_0^2 \epsilon^2 f^2 + R_0^2 \epsilon^2 f'^2}\, d\theta \\
\mathcal{S.E.} &= R_0 \sigma L \int_0^{2\pi} \sqrt{1 + 2\epsilon f + \epsilon^2 f^2 + \epsilon^2 f'^2}\, d\theta.
\end{aligned} \tag{3.6}$$

Now, using a taylor series of the form $\sqrt{1+\phi} = 1 + \frac{1}{2}\phi - \frac{1}{8}\phi^2 + \mathcal{O}(\phi^3)$, where $\phi = 2\epsilon f + \epsilon^2 f^2 + \epsilon^2 f'^2$. This taylor series is justified because $\epsilon \ll 1$, so ϕ is also very small, which yields

$$\begin{aligned}
\mathcal{S.E.} &= R_0 \sigma L \int_0^{2\pi} \left[1 + \epsilon f + \frac{1}{2}\epsilon^2 f^2 + \frac{1}{2}\epsilon^2 f'^2 - \frac{1}{8}\left(4\epsilon^2 f^2 + 4\epsilon^3 f^3 + 4\epsilon^3 f f'^2 + \epsilon^4 f^4 + 2\epsilon^4 f^2 f'^2 + \epsilon^4 f'^4 \right) \right] d\theta \\
\mathcal{S.E.} &= R_0 \sigma L \int_0^{2\pi} \left[1 + \epsilon f + \frac{1}{2}\epsilon^2 f'^2 + \mathcal{O}(\epsilon^3) \right] d\theta.
\end{aligned} \tag{3.7}$$

We assume no fluid is leaking or moving out of the droplet. Therefore, the volume of the droplet remains constant under deformation. As a result, one can express the volume of the deformed droplet to be equal to the volume of the undeformed droplet.

$$\frac{1}{2} L \int_0^{2\pi} R(\theta)^2\, d\theta = \pi R_0^2 L \tag{3.8}$$

Again, use (3.3) for $R(\theta)$, which yields

$$\begin{aligned}
\int_0^{2\pi} \left[R_0^2 + 2R_0^2\epsilon f + R_0^2\epsilon^2 f^2\right]\, d\theta &= 2\pi R_0^2 \\
\int_0^{2\pi} \left[1 + 2\epsilon f + \epsilon^2 f^2\right]\, d\theta &= 2\pi \\
\int_0^{2\pi} d\theta - 2\pi + \int_0^{2\pi} 2\epsilon f\, d\theta + \int_0^{2\pi} \epsilon^2 f^2\, d\theta &= 0 \\
\int_0^{2\pi} 2\epsilon f\, d\theta &= -\int_0^{2\pi} \epsilon^2 f^2\, d\theta.
\end{aligned} \tag{3.9}$$

Apply constraint (3.9) to ϵf in (3.7), in order to rewrite the surface energy as

$$\begin{aligned}
\mathcal{S}.\mathcal{E}. &= R_0\sigma L \int_0^{2\pi} \left[1 - \frac{1}{2}\epsilon^2 f^2 + \frac{1}{2}\epsilon^2 f'^2 + \mathcal{O}(\epsilon^3)\right]\, d\theta \\
\mathcal{S}.\mathcal{E}. &= R_0\sigma L \left(2\pi + \frac{\epsilon^2}{2}\int_0^{2\pi} \left[f'^2 - f^2\right]\, d\theta + \mathcal{O}(\epsilon^3)\right).
\end{aligned} \tag{3.10}$$

As mentioned in section section 3.1, f can be decomposed in harmonics, an expansion in $\cos(m\theta)$. More specifically, f can be written as

$$f(\theta) = \sum_{m=2}^{\infty} b_m \cos(m\theta). \tag{3.11}$$

The $\cos(m\theta)$ maintains the symmetry of the droplet and represents the deformation from the circular form of the droplet when looked at from the side (Fig. 4). The expansion coefficients b_m represent the amplitude of the perturbed perimeter at an angle $m\theta$.
The sum in (3.11) begins at $m = 2$ because $b_0 = 0$ and $b_1 = 0$. Now, $b_0 = 0$ because of volume conservation. Replace f in (3.9) by its decomposition given in (3.11) and observe that b_0 has to be zero, should the equility hold. Besides the constraint of volume conservation, we took the centre of our coordinate system to be at the center of mass of the deformed droplet. This constraint comes down to saying that the vertical coordinate integrated over the volume of the droplet is zero:

$$\begin{aligned}
\frac{1}{6}L\int_0^{2\pi} R(\theta)^3\cos(\theta)\, d\theta &= 0 \\
\frac{1}{6}L\int_0^{2\pi} \left(R_0^2 + 2R_0^2\epsilon f + R_0^2\epsilon^2 f^2\right)\left(R_0 + R_0\epsilon f\right)\cos(\theta)\, d\theta &= 0 \\
\frac{1}{6}L\int_0^{2\pi} \left[R_0^3 + 2R_0^3\epsilon f + R_0^3\epsilon^2 f^2 + R_0^3\epsilon f + 2R_0^3\epsilon^2 f^2 + R_0^3\epsilon^3 f^3\right]\cos(\theta)\, d\theta &= 0 \\
\int_0^{2\pi} \left[1 + 3\epsilon f + 3\epsilon^2 f^2 + \epsilon^3 f^3\right]\cos(\theta)\, d\theta &= 0 \\
\int_0^{2\pi} f\cos(\theta)\, d\theta &= -\int_0^{2\pi} \left[\epsilon f^2 + \frac{\epsilon^2 f^3}{3}\right]\cos(\theta)\, d\theta.
\end{aligned} \tag{3.12}$$

Again, replacing f in (3.12) by its decomposition given in (3.11) and it is clear that $b_1 = 0$. Physically, a change in the vertical position does not contribute to the growth of the perimeter and therefore the surface energy.

Using (3.11) and its derivative $f' = \sum_{m=2}^{\infty} b_m m(-\sin(m\theta))$ for f and f' in (3.10), yields

$$\mathcal{S}.\mathcal{E}. = R_0\sigma L\left(2\pi + \frac{\epsilon^2}{2}\sum_{m=2}^{\infty}\sum_{n=2}^{\infty} b_m b_n \int_0^{2\pi} \left[mn\sin(m\theta)\sin(n\theta) - \cos(m\theta)\cos(n\theta)\right]\, d\theta + \mathcal{O}(\epsilon^3)\right).$$

Realize that all integrals for which $m \neq n$ are equal to zero, because of orthogonality of the trigonometric terms. This kills all cross-terms in the sum leaving only the case for $m = n$, so

$$\begin{aligned}
\mathcal{S}.\mathcal{E}. &= R_0\sigma L\left(2\pi + \frac{\epsilon^2}{2}\sum_{m=2}^{\infty} b_m^2 \int_0^{2\pi} \left[m^2\sin^2(m\theta) - \cos^2(m\theta)\right]\, d\theta + \mathcal{O}(\epsilon^3)\right) \\
\mathcal{S}.\mathcal{E}. &= R_0\sigma L\left(2\pi + \frac{\epsilon^2}{2}\sum_{m=2}^{\infty} b_m^2 \left[-\frac{\left(m^2+1\right)\sin(4\pi m) - 4\pi m^3 + 4\pi m)}{4m}\right] + \mathcal{O}(\epsilon^3)\right).
\end{aligned}$$

Since m increases in integer steps, $\sin(4\pi m) = 0$ for all m, and we arrive at the final expression for the surface energy

$$\mathcal{S}.\mathcal{E}. = R_0\sigma L\left(2\pi + \frac{\epsilon^2}{2}\sum_{m=2}^{\infty} b_m^2\pi\left[m^2 - 1\right] + \mathcal{O}(\epsilon^3)\right). \tag{3.13}$$

Remember that (3.13) follows from (3.10), so we can conclude that the $\mathcal{O}(\epsilon^2)$ term always adds to the surface energy for every m possible. This reflects that the change of the shape of the droplet, $\int_0^{2\pi} f'^2$ in (3.13) and $\sum_{m=2}^{\infty} b_m^2\pi m^2$ in (3.10), adds to the perimeter length and thus the surface energy. This change of shape does not just add to the surface energy, it adds more than the term representing the shape of the substrate, $-\int_0^{2\pi} f^2$ in (3.13) and $-\sum_{m=2}^{\infty} b_m^2\pi$ in (3.10), can substract from the surface energy for every m.

3.3 Potential energy

In a field of gravity, the droplet with a mass naturally has a potential energy above some reference point. For our droplet, we choose this reference point to be the location of the substrate vertically below the droplet, where $\theta = 0$, just like Moláček and Bush did

$$\begin{aligned}
\mathcal{P}.\mathcal{E}. &= mgh \\
\mathcal{P}.\mathcal{E}. &= \pi R_0^2 L\rho g h
\end{aligned} \tag{3.14}$$

The height h is the height of the centre of mass of the droplet taken from our reference point. This can be decomposed into the height up to where $\theta = \alpha$, call this height Δ, and the height from Δ up to the centre of mass, which is $R(\alpha)\cos(\alpha)$. So we have $h = \Delta + R(\alpha)\cos(\alpha)$.
Now to calculate Δ for the case of $\Delta \ll R_2$, we get

$$\begin{aligned}
\left(R_2 - \Delta\right)^2 + \left(R(\alpha)\sin(\alpha)\right)^2 &= R_2^2 \\
R_2^2 - 2\Delta R_2 + \left(R(\alpha)\sin(\alpha)\right)^2 &= R_2^2 \\
\Delta &= \frac{R^2(\alpha)\sin^2(\alpha)}{2R_2}.
\end{aligned} \tag{3.15}$$

Combining (3.15) and $h = \Delta + R(\alpha)\cos(\alpha)$ and applying this to (3.14), we come to

$$\mathcal{P}.\mathcal{E}. = \pi R_0^2 L\rho g\left[R(\alpha)\cos(\alpha) + \frac{R^2(\alpha)\sin^2(\alpha)}{2R_2}\right]. \tag{3.16}$$

Take (3.3) and evaluate it at $\theta = \alpha$. Use this for (3.16), and realize that f in the following expression is evaluated at $\theta = \alpha$, gives

$$\mathcal{P}.\mathcal{E}. = \pi R_0^3 L\rho g \left[\cos(\alpha) + \frac{R_0}{2R_2}\sin^2(\alpha) + \epsilon f\cos(\alpha) + \frac{R_0}{R_2}\sin^2(\alpha)\epsilon f + \frac{R_0}{2R_2}\sin^2(\alpha)\epsilon^2 f^2\right].$$

Lastly, remember that we have $\mathcal{R} = 1 - \frac{R_0}{R_2}$, so we get

$$\mathcal{P}.\mathcal{E}. = \pi R_0^3 L\rho g \left[\cos(\alpha) + \epsilon f\left(\cos(\alpha) + (1-\mathcal{R})\sin^2(\alpha)\right) + \frac{1-\mathcal{R}}{2}\sin^2(\alpha) + \mathcal{O}(\epsilon^2)\right]. \tag{3.17}$$

It was already mentioned that δ is the relative contact area (3.4). We now average the potential energy over all the possible contact areas the droplet covers up to its actual contact area. The averaging is thus done over potential configurations of the substrate ranging from flat to its anticipated point of contact. The purpose of this is to let the droplet sit and feel the effects of the whole contact area, and not just the outline of the contact area. In our theory, this outline is found when the decomposition of f (3.11) is just plugged into (3.17) and one works with that potential energy. Physically, this outline for a cylindrical substrate represents some straight wire following the long axis direction of the cylindrical substrate. This averaging is done by performing the following integral on the potential energy

$$\overline{\mathcal{P}.\mathcal{E}.} = \frac{1}{\delta}\int_0^\alpha \mathcal{P}.\mathcal{E}.\, d\alpha'. \tag{3.18}$$

One can see here α' instead of α to indicate the difference between all the possible angles of last contact the droplet sits on and the actual angle of last contact, respectively.

Now apply the expansion in (3.11) to (3.17), and using α' instead of α to represent the potential configurations, which leads to the following expression

$$\mathcal{P}.\mathcal{E}. = \pi R_0^3 L\rho g \left[\cos(\alpha') + \epsilon\sum_{m=2}^{\infty} b_m\cos(m\alpha')\left(\cos(\alpha') + (1-\mathcal{R})\sin^2(\alpha')\right) + \frac{1-\mathcal{R}}{2}\sin^2(\alpha') + \mathcal{O}(\epsilon^2)\right]. \tag{3.19}$$

We restrict ourselves to a substrate close to a flat surface to get an approximate expression for the averaged potential energy. This means we can set $\mathcal{R} \approx 1$, so the two terms involving $\mathcal{R}$, the so called curvature terms, drop. This is also consistent with the earlier approximation that we made where $\Delta \ll R_2$. We do this to find a relation for b_m in section 3.4 to work with for the surface- and potential energy and future kinetic energy and dissipation. The effect of b_m on the droplet's shape for a slightly curved surface will also be seen there and this will show that b_m describes the droplet's shape on the substrate accurately, hence justifying the approximation to drop the curvature terms. Moláček and Bush also neglected the curvature term in their analogous expression for the potential energy, also because it is considered to be small (of $\mathcal{O}(\epsilon)$). This can be seen going from their eq. (18) to eq. (19). This does *not* mean that the curvature is completely gone from their and our calculations. The curvature $\mathcal{R}$ hides in δ or α, after all, the maximum contact area is approached when $\mathcal{R}$ goes to zero.

Performing (3.18) yields the final expression for the approximate averaged potential energy of the resting droplet

$$\overline{\mathcal{P}.\mathcal{E}.} \approx \pi R_0^3 L\rho g \left[\frac{1}{\delta}\int_0^\alpha \cos(\alpha')\, d\alpha' + \frac{\epsilon}{\delta}\sum_{m=2}^{\infty} b_m\left(\int_0^\alpha \cos(m\alpha')\cos(\alpha')\, d\alpha'\right)\right]$$

$$\overline{\mathcal{P}.\mathcal{E}.} \approx \pi R_0^3 L\rho g \left[\frac{\sin(\alpha)}{\delta} + \frac{\epsilon}{\delta}\sum_{m=2}^{\infty} b_m\left(\frac{\cos(\alpha)\sin(\alpha m)m - \sin(\alpha)\cos(\alpha m)}{m^2-1}\right)\right]. \tag{3.20}$$

3.4 Static deformation

When the droplet is resting on the substrate, it is in an equilibrium state with respect to its (free) variables, reflecting the fact that nature is "lazy". Hence, when calculating the sum of surface- and potential energy, any change with respect to their variables should be zero. Differentiating with b_m then yields

$$\frac{d}{db_m}\mathcal{S}.\mathcal{E}. + \frac{d}{db_m}\overline{\mathcal{P}.\mathcal{E}.} = 0.$$

Differentiating (3.13) and (3.20) with respect to b_m yields

$$R_0\sigma L\epsilon^2\pi b_m\left[m^2-1\right] + \frac{\pi R_0^3 L\rho g\epsilon}{\delta}\left[\frac{\cos(\alpha)\sin(\alpha m)m - \sin(\alpha)\cos(\alpha m)}{m^2-1}\right] \approx 0,$$

The approximate sign comes from the fact that we used the approximate averaged potential energy (3.20), where the curvature terms have been dropped. The above expression is an infinite set of equations, where a particular value for m is selected to calculate a specific b_m. Finally, we can express b_m as

$$b_m \approx -\frac{\mathbb{B}o}{\epsilon\delta}\left[\frac{\cos(\alpha)\sin(\alpha m)m - \sin(\alpha)\cos(\alpha m)}{\left(m^2-1\right)^2}\right], \qquad m \in [2,\infty)\,. \tag{3.21}$$

We already mentioned that b_0 and b_1 have to be zero, hence m starts at two and the above expression does not have a singularity at $m = 1$. The expansion coefficients b_m in (3.21) can be seen as the analogous equation of b_m found by Moláček and Bush in equation (20) of their article. This is thus the point where our theoretical development stops.
With our found b_m, we give some additional results: Remembering equation (3.4), the decomposition of f (3.11) can be written as

$$f(\theta) \approx -\frac{\pi\mathbb{B}o}{2\alpha\epsilon}\sum_{m=2}^{\infty}\left[\frac{\cos(\alpha)\sin(\alpha m)m - \sin(\alpha)\cos(\alpha m)}{\left(m^2-1\right)^2}\right]\cos(m\theta). \tag{3.22}$$

Consequently, we are also able to express the radius of the droplet (3.3) as

$$R(\theta) \approx R_0\left(1 - \frac{\pi\mathbb{B}o}{2\alpha}\sum_{m=2}^{\infty}\left[\frac{\cos(\alpha)\sin(\alpha m)m - \sin(\alpha)\cos(\alpha m)}{\left(m^2-1\right)^2}\right]\cos(m\theta)\right). \tag{3.23}$$

We can see that the radius of the droplet depends, essentially, on only two degrees of freedoms of the resting droplet system:

- The amount of gravity that is exerted on the droplet. This is represented by the Bond number $\mathbb{B}o$. Actually, δ also represents the amount of gravity that is exerted on the droplet. Imagine the droplet being "pulled" more towards the substrate with more gravity, hence an increase in relative contact area δ.
- The curvature of the substrate, which is hidden in α or analogously δ (3.4). One can think of keeping $\mathbb{B}o$ constant while changing α in (3.23), which can only be a consequence of a (small) change of curvature of the substrate.

We want to make clear that a relation between α (or δ) and $\mathbb{B}o$ and $\mathcal{R}$ might be found, like Moláček and Bush did. They found that $\delta = \frac{\mathbb{B}o}{3\mathcal{R}} + \mathcal{O}(\mathbb{B}o^{\frac{3}{2}})$, where δ now both encorporates the curvature of the substrate through $\mathcal{R}$ and the gravity through $\mathbb{B}o$. A similar expression may be found by following the same derivations they give in equations (6) through (13) for our one-dimensional system, but that is not done in this thesis due to time constraints.

3.5 Results

We first want to show the effect and necessity of the averaging procedure (3.18) on the potential energy for the shape of the resting droplet. This is done by plotting the radius (3.23) on a near flat surface as a function of its angle θ, at a certain value of $\mathbb{B}o$ and α. These $\mathbb{B}o$ and α are chosen such that the droplet has an approximate flat base, and thus a near flat substrate must be underneath it. The results can be seen in Fig. 5. One can see that, for an high enough $\mathbb{B}o$, the droplet's contact area conforms to the near flat surface if the potential energy is averaged over (3.18). If this averaging procedure is not done, the contact area between $\theta = \alpha$ and $\theta = -\alpha$ is not "felt"by the droplet, as the area over which the reaction force of gravity works on the droplet is not felt. As a result, the droplet is pulled below the area where there should be a surface between $\theta = \alpha$ and $\theta = -\alpha$, as if the droplet only rested on two straight wires at $\theta = \alpha$ and $\theta = -\alpha$.

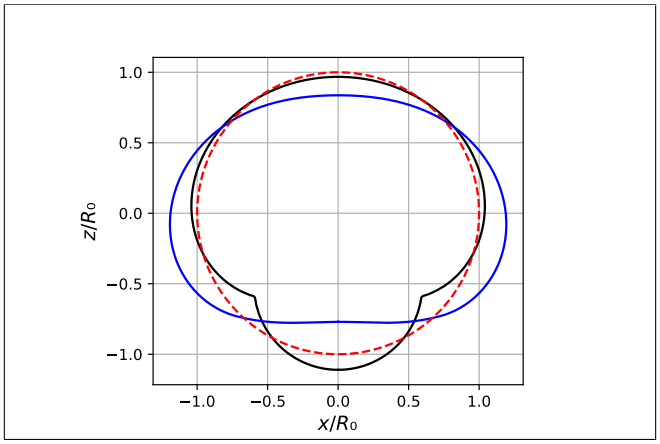

Figure 5: A droplet resting on a near flat surface for $\mathbb{B}o = 0.625$ and $\alpha = \frac{\pi}{4}$. The reaction force for the droplet represented by the black line is performed by two straight wires at the angle of last contact α. The reaction force for the droplet represented by the blue line is generated by the whole contact area as a consequence of the averaging procedure 3.18, ranging from $\alpha' \in [0, \alpha]$.

We can also see how the droplet behaves for the b_m found using the approximate averaged potential energy (3.20). The behavior can be seen in Fig. 6.

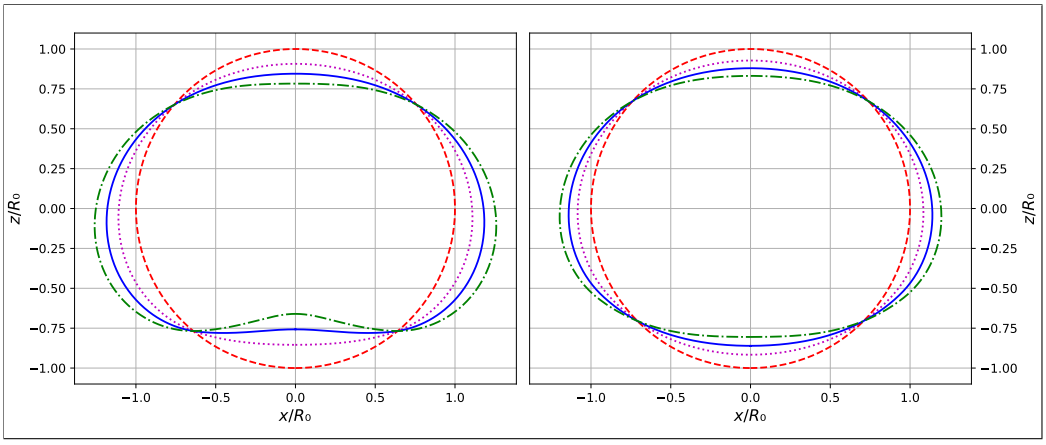

Figure 6: A droplet resting on a surface for $\alpha = \frac{\pi}{4}$ (lefthand side) and $\alpha = \frac{\pi}{3}$ (righthand side) at different $\mathbb{B}o$. The red dashed line indicates the undeformed droplet, so $\mathbb{B}o = 0$. The purple dotted line represents the deformed droplet at $\mathbb{B}o = 0.375$. The blue solid line represents the deformed droplet at $\mathbb{B}o = 0.625$ and the green dashed-dotted line at $\mathbb{B}o = 0.875$.

We can see in Fig. 6 that the droplet is symmetrical around $x = 0$, which is expected. Also for higher $\mathbb{B}o$, the droplet is compressed more and thus expands more to the left and right on the scaled x-axis.

Let us look at the case when $\alpha = \frac{\pi}{4}$ in more detail. We see the droplet moving towards a flat base for higher $\mathbb{B}o$ until $\mathbb{B}o \approx 0.625$, being pulled towards the substrate with a stronger gravitational force. For $\mathbb{B}o$>0.625, we see the droplet moving away from a flat base, indicating that the averaging procedure for the potential energy on this substrate will become a less accurate approximation for the droplet's shape.
For the case when $\alpha = \frac{\pi}{3}$, we see that for the same values of $\mathbb{B}o$ the droplet is not compressed as much compared to $\alpha = \frac{\pi}{4}$. This also means that the droplet moves slower towards a flat base for increasing $\mathbb{B}o$ compared to the case when $\alpha = \frac{\pi}{4}$. Consequently, at higher (or lower) α compared to some reference α, the averaging procedure of the potential energy is accurate until higher (or lower) values of $\mathbb{B}o$.

Like we indicated before, a relation can be found beween α and $\mathbb{B}o$ depending on the curvature, but that is not done in this thesis. Therefore, we cannot tell how the substrate is curved for different α and $\mathbb{B}o$. All that we know is that this curvature is small and, specifically, for a flat based droplet, the substrate must be nearly flat.

When the angle of last contact is $\alpha = \frac{\pi}{3}$, the behavior of the droplet is accurate until $\mathbb{B}o \approx 1.167$. This can be seen in Fig. 7.

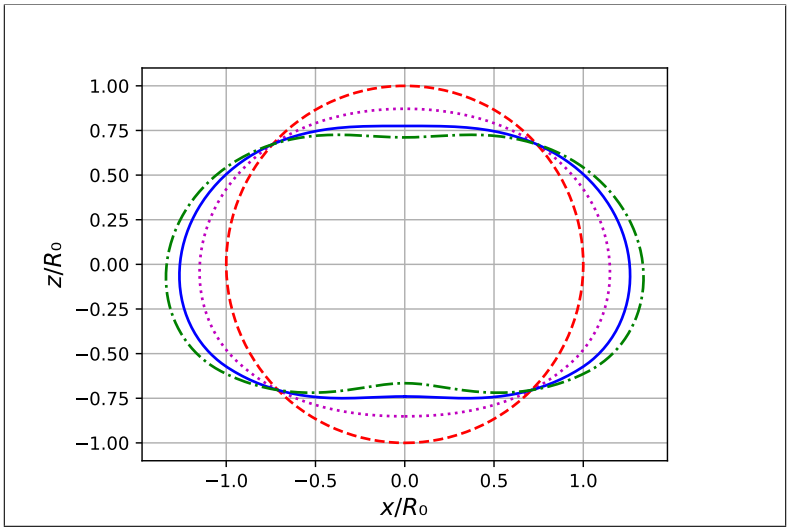

Figure 7: A droplet resting on a flat surface for $\alpha = \frac{\pi}{3}$ at different $\mathbb{B}o$. The red dashed line indicates the undeformed droplet, so $\mathbb{B}o = 0$. The purple dotted line represents the deformed droplet at $\mathbb{B}o = \frac{2}{3} = 0.667$. The blue solid line represents the deformed droplet at $\mathbb{B}o = \frac{7}{6} = 1.167$ and the green dashed-dotted line at $\mathbb{B}o = \frac{3}{2} = 1.5$.

These results prove that the found b_m describes the droplet's shape accurately on a slightly curved surface, because we assumed $\Delta \ll R_2$. Therefore, this b_m can be used in future work when calculating the kinetic energy and dissipation in the droplet when impacting at $\mathbb{W}e \ll 1$ on a slightly curved rigid surface.

3.6 Guide to completion

Since we have finished our theoretical development, we now want to give the interested reader a short guide on how to complete the one-dimensional theory, in order to be able to rationalize the bouncing- and walking droplet's behaviour. The steps given below serve as a guide through the three subsequent papers published by Moláček and Bush mentioned at the beginning of section 3:

- As indicated before, now that we have calculated the surface and potential energy in terms of b_m, the next steps are to calculate the kinetic energy and dissipation in the droplet. The time-dependence of the droplet's deformation is then also introduced by a time-dependent *effective* gravitational force acting on the droplet. A Lagrangian can be constructed from these energies, which can be used to construct the equation of motion of the quasi-static droplet. Specifically, the center of mass position and shape variations as a function of time. This has to be adjusted to represent the dynamics and eventual equation of motion of the centre of mass when a droplet impacts the surface of a liquid bath. First, switch to impacts at moderate Weber number ($0.01<\mathbb{W}e\lesssim 1$), because the droplet is not just sitting on the bath, it has an incoming impulse. Then, one must simplify the real liquid bath shape to be of quasi-static form and deform in the same order of magnitude as the droplet over time. This is the model basis Moláček and Bush use in their second article to derive the equation of motion of the bouncing droplet, called the *logarithmic spring model* (see p. 607-609 in [13]). Hence our development and the given adjustments above will lead to an analogous logarithmic spring model for our one-dimensional system. This logarithmic spring model rationalizes the bouncing dynamics and thus the effective influence of the bath on the vertical dynamics of the droplet in the correct parameter regime.

- The next interesting step is to develop a theory for the walking regime of the droplet, where the logarithmic spring model, as developed, is not valuable anymore. Firstly, the evolution of the standing waves created by a drop impact over time and in space on the liquid bath must be derived for the one dimensional theory. The two-dimensional version is derived in section 3 of the third article by Moláček and Bush [7]. This is done through considering a single drop impact with the effect of creating a standing wave. It is assumed that the shape of the standing waves at a certain time can be given through addition of all previous drop impacts and their resulting standing waves. They found that an impact creates a standing wave with nearly sinusoidal time dependence and Bessel function spatial dependence, which decays exponentially in time. For our one-dimensional bath the standing waves can only move left or right and not radially away from a drop impact like in the two-dimensional bath. The decaying height of the wave away from the point of impact will thus not be as strong in the one-dimensional bath as it is in the two-dimensional bath, as it will lack geometrical spreading. We predict that this Bessel function will be replaced by an other (simpler) function, a moderately decaying sinusoidal function.
  In section 4 of the third article, by considering all the relevant forces acting on the droplet, they obtain a consistent model for the droplet's horizontal dynamics, resulting in a trajectory equation for the horizontal position of the droplet. One has to consider the horizontal drag during contact with the bath and the horizontal drag during flight. Also, the horizontal momentum the droplet gets from the wave it lands on has to be given in terms of the system's parameters to get to a trajectory equation.

Some derivations are being supplemented by numerical considerations or fitting parameters to experiments done with the walkers in all three articles. Coincidentally, this was not needed for our development yet. So in order to find a trajectory equation and the logarithmic spring for our one-dimensional system, one has to supplement it with experiments on the system portrayed in Fig. 3.
Lastly, it must be stressed that the walker system is highly sensitive to which parameter regime it is looked at. For example, the logarithmic spring model only works for moderate to low Weber numbers ($\mathbb{W}e\lesssim 3$). Always keep in mind through what lens one is looking with respect to the parameters of the system in the development of the theory, in order to have the theory rationalize the reality of how the droplet behaves.

4 Conclusion and Discussion

In conclusion, we have derived the surface- and potential energy in terms of expansion coefficients b_m of a quasi-static droplet in the one-dimensional system. In the same system, the shape of a resting droplet is derived. Adding to and adjusting these results for a correct parameter regime will lead to the equation of motion of the vertically bouncing droplet in the one-dimensional system.

There are a couple of points that require further discussion. First of all, we assumed in deriving (3.15) that $\Delta \ll R_2$. This assumption becomes less accurate when the contact area approaches the maximum contact area so that the curvature terms cannot be neglected in (3.19). Hence the approximate averaged version of the potential energy (3.20) and consequently the expression for b_m become less realistic. Subsequently, this found b_m then is used to describe the complete surface- and potential energy, (3.13) and (3.17), which become less realistic too. This would break down the model.
Secondly, one may wonder why we have restricted ourselves to a *slightly* curved substrate. We wanted to maintain the analogy to the derivation of Moláček and Bush to preserve continuity in the development of our one-dimensional theory, which is the eventual goal. The reader is invited to further investigate what happens when the approximation $\Delta \ll R_2$ is not made, which results in nonlinear effects becoming important at impact of the droplet.
Thirdly, it is interesting to understand why the averaging procedure of the potential energy is accurate up to higher values of $\mathbb{B}o$ for increasing α. Gravity exerts a reaction force through the underlying substrate on the droplet. One can imagine the reaction force has a larger area to spread out this force on the droplet for increasing α, which upholds the accuracy of the averaging method longer. Or the increase of the actual contact area "asks"the droplet to deform more with the same amount of gravity, which is the same as an increase in Bond number (3.2). Improving on the averaging method or finding another way to make the droplet feel the whole contact area and to consequently find a different b_m might be interesting for future research.

In Section 2, we examined the walker system behavior in a bath where standing waves appear due to wave interference as a droplet bounces on or walks across the bath. But now, take the bath to be very big so that the system can be seen as an open system without boundaries. It is interesting to speculate what will happen in such a system to a bouncing droplet. When perturbed in some direction, will the droplet be continuing on a straight line, will it deflect its path, or will it randomly start hopping to the left and right on that same directional line? When this is the case, what will be the difference in behaviour in such a system to that in our one-dimensional system (Fig. 3)? Then also, can there be or how does the chaotic behavior look like without boundaries? Since quantum particles also exhibit statistical behaviour in the absence of boundaries, these questions are interesting to be looked at for future work.

5 Thoughts on quantum interpretations

The choice for the subject of this thesis was inspired by my and my supervisors' interest in the fundamental meaning of quantum mechanics. So I like to explain my present thoughts and beliefs on quantum interpretations. In order for me to do this, I cannot merely base these interpretations on my logical mind. Incorporating my fundamental experience of reality according to my highest truth at this moment can only make for a right answer.

When my mind slows down and the immediacy of life comes into play, some mist is lifted and a connection with the world around is made that shifts my idea that physics is the only true description of reality. Coincidences are no more, bliss is not just a chemical reaction and the law of attraction is not a mathematical description of gravity. One may argue that these experiences are mere tricks of the brain, but direct experience, as the mind could never, convinces me otherwise. Therefore, I belief there are forces in our world that can never be perceived by only using physics as a way of observing them. As a result, I cannot exclude the possibility that other forces determine the outcome of quantum statistics without us being able to tell how and why. But I suspect that these other forces will not appear in the description that physics gives to reality.

Let me leave these mystic forces behind and see the world through the powerful lens of physics, which is close to my hart. There is still room, be it small, for hidden variable theories which would be compatible with quantum mechanics. The deterministic chaotic pilot-wave dynamics certainly has its shortcomings as an hidden variable theory, but it augments what I think to be unique in quantum mechanics. Consequently, I cannot exclude the possibility of dynamical phenomena going on at the Planck scale that explain the probabilistic results found in quantum mechanics. But I also see it likely that our evolved classical intuition cannot comprehend the abstract reality of quantum mechanics. After all, we connect with the world around us on such a different scale that the reality of the quantum realm may not be for us to fully understand. Following this line of arguing, we must come to realize that we can only understand quantum mechanics if we admit that our idea of fully understanding it is not compatible with reality. After all, meeting reality on reality's terms is all what physics is about, right?

References

[1] J. W. M. Bush. "Pilot-wave hydrodynamics". In: *Annu. Rev. Fluid Mech.* 47 (2005), pp. 269–292.

[2] M. Faraday. "On the forms and states of fluids on vibrating elastic surfaces". In: *Philos. Trans. R. Soc. Lond.* 121 (1831), pp. 319–340.

[3] Y. Couder, S. Protière, and E. Fort et al. "Walking and orbiting droplets". In: *Nature* 437 (2005), p. 208.

[4] J.W.M. Bush et al. "Introduction to focus issue on hydrodynamic quantum analogs". In: *Chaos* 28.096001 (2018).

[5] A. Eddi et al. "Unpredictable tunneling of a classical wave– particle association". In: *Phys. Rev. Lett.* 102.24041 (2009).

[6] Ø. Wind-Willassen et al. "Exotic states of bouncing and walking droplets". In: *Phys. Fluids* 25.082002 (2013).

[7] J. Moláček and J. W. M. Bush. "Drops bouncing on a vibrating bath: towards a hydrodynamic pilot-wave theory". In: *J. Fluid Mech.* 727 (2013), pp. 612–647.

[8] D.M. Harris et al. "Wavelike statistics from pilot-wave dynamics in a circular corral". In: *Phys. Rev. E* 88.011001 (2013).

[9] T. Cristea-Platon, P.J. Sáenz, and J.W.M. Bush. "Walking droplets in a circular corral: Quantisation and chaos". In: *Chaos (Focus Issue: Hydrodynamic Quantum Analogs)* 28.096116 (2018).

[10] M.F. Crommie, C.P. Lutz, and D.M. Eigler. "Confinement of electrons to quantum corrals on a metal surface". In: *Science* 262 (1993), pp. 218–220.

[11] G.A. Fieta and E.J. Heller. "Theory of quantum corrals and quantum mirages". In: *Rev. Mod. Phys.* 88 (2003), pp. 933–948.

[12] J. Moláček and J. W. M. Bush. "A quasi-static model of drop impact". In: *Phys. Fluids* 24.127103 (2012).

[13] J. Moláček and J. W. M. Bush. "Drops bouncing on a vibrating bath". In: *J. Fluid Mech.* 727 (2013), pp. 582–611.

[14] S.E. Turton, M.M.P. Couchman, and J.W.M. Bush. "A review of the theoretical modeling of walking droplets: Toward a generalized pilot-wave framework". In: *Chaos (Focus Issue: Hydrodynamic Quantum Analogs)* 28.096111 (2018).

[15] A.K. Chesters. "An analytical solution for the profile and volume of a small drop or bubble symmetrical about a vertical axis". In: *J. Fluid Mech.* 81 (1977), pp. 609–624.